Metabolic regulation and glucose sensitivity of cortical radial glial cells

Brian G. Rash[a], Nicola Micali[a], Anita J. Huttner[a,b], Yury M. Morozov[a], Tamas L. Horvath[a,c,d], and Pasko Rakic[a,d,1]

[a]Department of Neuroscience, Yale School of Medicine, New Haven, CT 06520; [b]Department of Pathology, Yale School of Medicine, New Haven, CT 06520; [c]Section of Comparative Medicine, Yale School of Medicine, New Haven, CT 06520; and [d]Kavli Institute for Neuroscience, Yale School of Medicine, New Haven, CT 06520

Contributed by Pasko Rakic, August 14, 2018 (sent for review May 10, 2018; reviewed by Jens Brüning, Zoltan Molnar, and Nicolas C. Spitzer)

The primary stem cells of the cerebral cortex are the radial glial cells (RGCs), and disturbances in their operation lead to myriad brain disorders in all mammals from mice to humans. Here, we found in mice that maternal gestational obesity and hyperglycemia can impair the maturation of RGC fibers and delay cortical neurogenesis. To investigate potential mechanisms, we used optogenetic live-imaging approaches in embryonic cortical slices. We found that Ca^{2+} signaling regulates mitochondrial transport and is crucial for metabolic support in RGC fibers. Cyclic intracellular Ca^{2+} discharge from localized RGC fiber segments detains passing mitochondria and ensures their proper distribution and enrichment at specific sites such as endfeet. Impairment of mitochondrial function caused an acute loss of Ca^{2+} signaling, while hyperglycemia decreased Ca^{2+} activity and impaired mitochondrial transport, leading to degradation of the RGC scaffold. Our findings uncover a physiological mechanism indicating pathways by which gestational metabolic disturbances can interfere with brain development.

radial glia | calcium | mitochondria | metabolic disorders | stem cell

Radial glial cells (RGCs) perform several key functions during cortical development. Firstly, they are the primary stem cell of the cerebral cortex, systematically generating all of its excitatory neurons. Following neurogenesis, neuronal migration along the elongated fibers of RGCs to specific areal and laminar destinations in the developing cortical plate brings neurons to their final resting places where they generate circuits (1–4). Subsequent neuronal maturation and integration of synaptic circuitry is a function of genetic and activity-dependent processes (5–7) and is highly dependent on proper cell position (8).

Genetic errors within RGCs in many signaling pathways such as Notch or fibroblast growth factors (FGFs) cause a range of deficits in mouse and human cortical development, with severe outcomes including microcephaly, lissencephaly, ventriculomegaly, holoprosencephaly, changes in the patterning of the functional area map, and many other syndromes (9–12). Likewise, neuronal displacement involving failed or improper migration can be caused by defects in RGC function triggered by a variety of genetic mutations and can lead to neurodevelopmental disorders of the cerebral cortex with consequent lifelong cognitive impairments (12, 13). However, the role of various environmental factors in disrupting RGC physiology and function in utero remains far from clear. One key example is the finding that maternal inflammation is a source of disrupted RGC function with consequences for fetal neurogenesis (14).

Gestational metabolic disorders are on the rise, and a connection with cognitive developmental disorders has been reported (15). Gestational diabetes rates were estimated at between 4.6% and 9.2% in the United States in 2010 and rising along with the obesity rate (>40% among US women in 2010) (16), and fetal hyperglycemia is a chief cause of numerous adverse outcomes in infants (17, 18). Interestingly, cases of autism spectrum disorder (ASD) are estimated to be about 60% comorbid with mitochondrial disease or other metabolic disorders (19–22), and there is some evidence of comorbidities such as malpositioned cortical neurons indicative of failed migration. However, the cellular mechanisms under metabolic pressure impacting the prenatal development of the cerebral cortex are not understood.

The elongated fibers of RGCs are critical not only for directed excitatory neuronal migration to the cortical plate (1), but also for the communication of important developmental signals via protein and mRNA transport along their length, which in turn impacts RGC proliferation and neurogenesis (23, 24). Thus, the intracellular machinery regulating such transport determines whether such signals will be able to correctly modulate these processes. Calcium signaling is one mechanism that is able to modify organelle transport, enzymatic activity, downstream growth factor signaling pathways such as the FGF pathway, growth cone behavior, and cytoskeletal dynamics in many cell types, and it is a key feature of neural development (25–27). Indeed, a diverse landscape of patterned Ca^{2+} activities within RGCs and newborn neurons has become evident, offering clues to the physiology of RGCs and their long fibers (28, 29). For example, epochs of rapid Ca^{2+} bursting activity in RGCs coincide with the initiation of radial neuronal migration, are abolished by constitutive Notch signaling, and indeed may be required for neuronal differentiation (28). Bidirectional Ca^{2+} signals have also been reported to propagate between the postmitotic cortical plate and progenitor zones, indicating communication and feedback that regulate Ca^{2+} tone in RGC somata and their proliferation (28). Here, we sought to establish whether identifiable changes in RGC structure or physiology are associated with maternal metabolic disorders during gestation as well as in live brain-slice experiments.

Significance

Metabolic abnormalities during gestation have been previously linked to increased likelihood of dyslexia, autism, and attention deficit hyperactivity disorder, but the factors involved and how they may act during cortical development is unknown. Here, we found in rodents that obesity and hyperglycemia affect the primary stem cells of the cortex (radial glial cells), reducing their ability to perform neurogenesis and form the radial scaffold needed for neuronal migration. At the subcellular level, excess glucose degraded calcium activity and the transport of mitochondria in the radial scaffold. Consequent delayed neuronal production and migration were observed. These results reveal aspects of neurogenesis as well as the sensitivity of the cortical development process to certain gestational metabolic influences.

Author contributions: B.G.R., N.M., A.J.H., Y.M.M., T.L.H., and P.R. designed research; B.G.R., N.M., A.J.H., and Y.M.M. performed research; B.G.R. contributed new reagents/analytic tools; B.G.R., N.M., and Y.M.M. analyzed data; and B.G.R. and P.R. wrote the paper.

Reviewers: J.B., Max Planck Institute for Metabolism Research, Cologne; Z.M., University of Oxford; and N.C.S., University of California, San Diego.

The authors declare no conflict of interest.

[1]To whom correspondence should be addressed. Email: pasko.rakic@yale.edu.

This article contains supporting information online at www.pnas.org/lookup/suppl/doi:10.1073/pnas.1808066115/-/DCSupplemental.

Published online September 17, 2018.

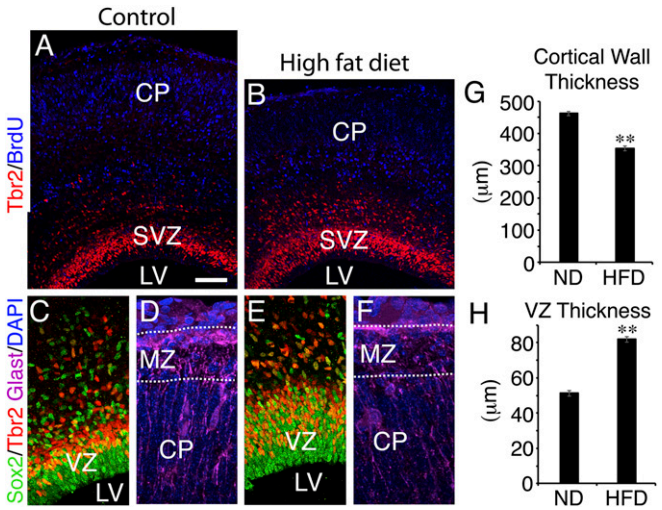

Fig. 1. Gestational obesity delays cortical neurogenesis and impairs radial fiber maturation. Coronal sections of E17.5 CD1 cortex ($n = 4$) from normal-diet (ND) mothers (*A*, *C*, and *D*) compared with embryos ($n = 4$) from HFD obese, hyperglycemic mothers (*B*, *E*, and *F*) stained for the RGC marker Sox2, the SVZ marker Tbr2, BrdU (E12.5 injection), or GLAST, a marker of RGCs and presumptive astrocytes. Cortical wall thickness was reduced (*G*), while the progenitor layers were increased in thickness (*H*). The presence of $BrdU^+$ presumptive neurons in the cortical plate (CP) of HFD embryos also appeared to be reduced (*A* and *B*), and RGC basal fibers showed disorganized and immature pial endfoot projections in the marginal zone (MZ). *A* is a composite of two images. (Scale bar: 100 μm in *A* and *B*; 50 μm in *C* and *E*; 20 μm in *D* and *F*.) Error bars represent SEM. $^{**}P < 0.0001$. LV, lateral ventricle.

Results

Impaired Radial Fiber Maturation and Delayed Neurogenesis in Gestational Obesity. It was previously shown in humans that the offspring of mothers with gestational obesity have an increased likelihood of cognitive developmental disorders such as autism, dyslexia, and attention deficit hyperactivity disorder (15). The offspring of mice with gestational obesity due to a high-fat diet (HFD) have delayed brain development, and the defects are attributed to effects on the embryo rather than an altered uterine environment (30). However, whether cortical development is impaired because of abnormalities in cortical progenitor cell physiology and function is unknown. We exposed female mice to an HFD containing 45% calories from fat for a period of 3 mo. As expected, about half of these animals developed severe obesity and hyperglycemia (337.0 ± 22.6 mg/dL blood glucose during a glucose tolerance test; $n = 16$). Severely obese HFD animals (weighing over 60 g) were selected for breeding, and the brains of their offspring were compared with those of normal-diet control females weighing less than 30 g. A pulse of BrdU (50 mg/kg) was given at embryonic day (E)12.5 to label neurons produced at that time, and the embryos were analyzed at E17.5. We found that, as reported previously (30), the telencephalon was reduced in size, particularly with regard to cortical wall thickness (Fig. 1 *A*, *B*, and *G*). Using immunohistochemistry for Sox2, Tbr2, and BrdU, we found an increase in the thickness of the ventricular zone (VZ) and the subventricular zone (SVZ) (Fig. 1 *C*, *E*, and *H*), and a substantial increase in the ratio of RGCs to postmitotic cortical neurons was evident. These data indicate a change in the proliferation/differentiation dynamics of RGCs and are consistent with a reduction in neuronal differentiation. Analysis of cell death by activated Casp3 immunohistochemistry did not indicate any apparent change (*SI Appendix*, Fig. S1 *A* and *B*). However, we noted that RGC basal fibers, which normally project to the marginal zone and bifurcate or otherwise radiate multiple endfoot projections to the pial surface, showed less developed basal endfoot projections in HFD offspring (Fig. 1 *D* and *F*). Determining how the numerous obesity-related changes in metabolism could affect cortical progenitors is a complex problem (31), but one chief concern is the diminished ability to regulate blood glucose. Therefore, we investigated whether hypo- or hyperglycemia could interfere with RGC development and function.

Ca^{2+} Regulation of Mitochondrial Transport in RGCs. Mitochondria are key metabolic compartments and regulators of cellular signaling and transport systems, including endoplasmic reticulum (ER)-based Ca^{2+} signaling in many cell types, and are thought to associate with ER through mitochondria-associated membrane linkages (32–35). The recent discovery of Ca^{2+} activity as a major dynamic feature of RGC fibers hints at a possible role in RGC homeostasis and function (Movie S1) (28). To examine how gestational glucose changes could affect cortical progenitors, we first performed a detailed analysis of the subcellular dynamics of RGCs in cortical slices, focusing on mitochondrial transport in relation to Ca^{2+} signaling.

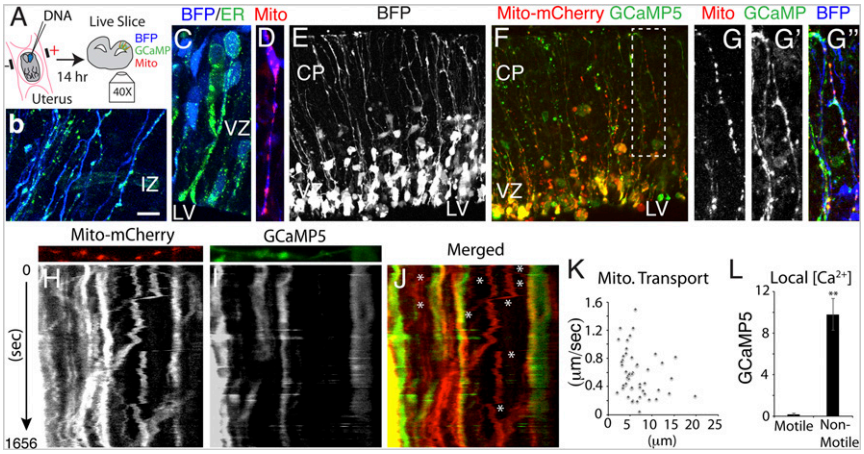

Fig. 2. Inverse relationship between Ca^{2+} activity and mitochondrial transport. (*A*) Schematic of an in utero electroporation videomicroscopy experiment. (*B* and *C*) ER is present throughout RGC somata, fibers, and endfeet, as indicated by direct fluorescence of ER-targeted EGFP ($n = 3$ embryos). (*D–J*) Mitochondria were labeled with Mito-mCherry (*D*), along with cytoplasmic BFP and GCaMP5 (*E–G*), and their transport was monitored by live imaging in relation to Ca^{2+} signaling and displayed as dual-color kymographs ($n = 19$ slices from 12 embryos) (*H–J*). *G* is a high magnification view of the boxed region in *F*. (*K*) Mitochondrial transport rates and distances are presented as a scatterplot ($n = 47$ mitochondria from $n = 3$ embryos). Mitochondrial transport was more rapid where $[Ca^{2+}]$ was lower (*J*, asterisks, and *L*, $n = 39$). (Scale bar: 10 μm in *B–D* and *H–J*; 50 μm in *E* and *F*.) $^{**}P < 0.0001$.

The source of most Ca^{2+} dynamic activity in RGCs is the ER (28, 29). To determine the overall distribution of ER in individual RGC fibers, we electroporated an ER-targeted EGFP plasmid in utero at E14.5 together with blue fluorescent protein (BFP), and performed imaging after a 14-h survival period (Fig. 2*A*). We detected abundant ER within RGC somata and throughout apical and basal RGC fibers, including apical and basal endfeet (Fig. 2 *B* and *C*), providing Ca^{2+} stores at almost any position within RGC fibers.

To visualize mitochondria and determine how Ca^{2+} signaling integrates with mitochondrial function in RGC fibers, we electroporated a mitochondria-targeted mCherry plasmid in utero at E14.5 together with plasmids encoding BFP and GCaMP5. Combined with confocal videomicroscopy, we monitored the transport of individual mitochondria in RGC fibers in live embryonic brain slices in relation to Ca^{2+} dynamic events originating within individual RGC fibers. We found that mitochondria were abundant in RGC somata, as well as their apical and basal fibers, and were enriched in endfeet (Fig. 2 *D*, *F*, and *G*). We observed rapid anterograde and retrograde mitochondrial transport in RGC fibers as well as some stationary mitochondria (0.53 ± 0.04 μm/s; mean transport distance, 6.58 ± 0.51 μm; $n = 64$; Fig. 2 *H*, *J*, and *K* and Movie S2), similar to neuronal dendrites and axons (36, 37). Stationary mitochondria could be tethered to ER or the plasma membrane, derailed from their microtubule track, or associated with inactive transport machinery. Consistent with a role for Ca^{2+} in the inhibition of mitochondrial transport, we observed lower transport rates within RGC fiber segments with high Ca^{2+} in movies and in dual kymographs representing mitochondrial transport and Ca^{2+} concentration (Fig. 2 *H–J*, and *L* and Movies S3 and S4). Since ∼90% of all mitochondria in RGC fibers were motile, it appears that mitochondria are typically unattached to the plasma membrane or nonmotile ER, although it is possible that small packets of ER remain attached to mitochondria during transport.

To determine whether mitochondrial activity can regulate patterned Ca^{2+} activity of RGCs, we exposed electroporated slices to inhibitors of aerobic respiration. Application of carbonyl cyanide *m*-chlorophenyl hydrazone (CCCP), a proton ionophore that disrupts the proton gradient (32, 38, 39), abolished large-amplitude Ca^{2+} dynamic activity (above twofold ΔF/F) within a few seconds (Fig. 3 *A–D* and *G*; *SI Appendix*, Fig. S2; and Movies S5 and S6). This short-latency effect suggests a close interaction between mitochondrial function and intracellular Ca^{2+} dynamic activity within RGC fibers. After several minutes of exposure, Ca^{2+} levels were increased in RGC fibers, consistent with the hypothesis that mitochondrial function is needed for ER Ca^{2+} import from the cytoplasm. In addition, CCCP abolished both anterograde and retrograde mitochondrial shuttling through RGC fibers (Fig. 3 *E*, *F*, and *H*; compare Movie S7, control with Movie S8, +50 μM CCCP), likely due to both the long-latency Ca^{2+} rise and sustained loss of ATP synthesis. These data indicate that the mitochondrial proton gradient is needed for maintaining Ca^{2+} dynamic activity in RGCs and that it is necessary for mitochondrial shuttling in RGC fibers, likely in part due to local ER-based Ca^{2+} regulation. Thus, we identify an ER-based Ca^{2+} feedback mechanism ensuring the proper shuttling, localized retention, and dispersion of mitochondria throughout the RGC scaffold during the period of cortical neurogenesis and migration.

Ca^{2+} Signaling and Mitochondrial Transport Are Degraded by Hyperglycemia. Using our optogenetic videomicroscopy system, we modeled hypo- and hyperglycemia in cortical slices by varying the dextrose concentration in artificial cerebrospinal fluid (ACSF) and characterized the response of cortical RGCs. We labeled cortical RGCs with BFP, GCaMP5, and Mito-mCherry using in utero electroporation at E14.5, prepared live slices 14 h later, and measured changes in patterned Ca^{2+} activity, mitochondrial transport, and RGC scaffold structure due to variations in glucose levels.

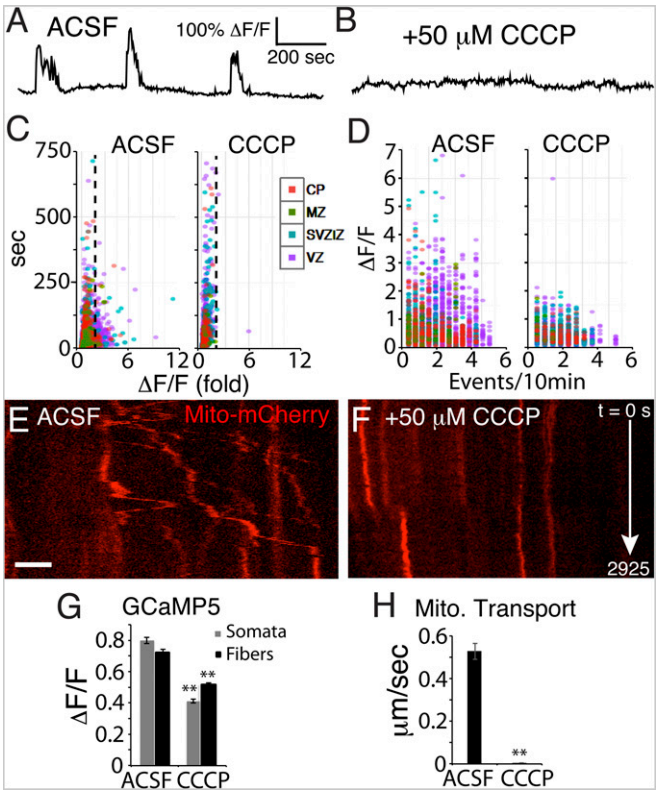

Fig. 3. Mitochondrial function is needed for Ca^{2+} dynamic activity and mitochondrial motility in RGCs. (*A–G*) Optically recorded Ca^{2+} dynamic activity in RGCs was severely reduced by the protonophore CCCP. (*A* and *B*) Optogenetic GCaMP5 signal traces from a single RGC illustrate Ca^{2+} activity silencing by CCCP. The largest Ca^{2+} events, above twofold ΔF/F (dotted line), were abolished by CCCP exposure (*C*); many small-amplitude/long-duration "events" are detected by MATLAB due to movement artifacts in ROIs of the slice movie. High-frequency/high-amplitude events were reduced in number (*D*); $n = 2{,}830$ RGC control Ca^{2+} events and $n = 1{,}971$ CCCP Ca^{2+} events; $n = 3$ slices. Mitochondrial transport was also severely reduced (kymographs in *E*, *F*, and *H*); $n = 64$ control and $n = 77$ CCCP mitochondria analyzed; $n = 3$ slices. (Scale bar: 10 μm in *E* and *F*.). $^{**}P < 0.0001$

Normal human fetal blood glucose levels in midgestation are ∼5 mM and are often 10 to 20 mM in hyperglycemia (40). However, a key parameter is the intracellular glucose concentration in RGCs, which has never been measured in human fetuses. In utero, the composition of fetal blood and embryonic CSF is not well understood, but GLUT4 glucose transporters utilize insulin to increase cellular glucose uptake from the blood and are found in brain neuroepithelium after E9 in rats (41). In a cortical-slice environment, RGCs are deprived of insulin, suggesting that the intracellular glucose concentration of RGCs in slices bathed in ACSF could be different from in utero. Thus, we explored the glucose dependence of RGCs by utilizing a range of glucose concentrations (0, 5, 10, and 40 mM) in a controlled ACSF environment.

We found that the RGC scaffold substantially retracts within 3 h of exposure to 40 mM glucose levels, while RGC fibers were much more stable within the euglycemic range (Fig. 4 *A–G*). Calcium activity in RGCs bathed in ACSF containing 0 mM glucose severely declined in both amplitude and frequency within a few minutes, after which most cells showed no detectable Ca^{2+} activity (*SI Appendix*, Fig. S3), indicating acute dependence on extracellular glucose. Compared with 5 mM glucose, Ca^{2+} activity at 10 mM showed a slight but nonsignificant decline in amplitude, yet a substantial decline in frequency, and we observed a major reduction in both amplitude and frequency at 40 mM (Fig. 4 *H–K*

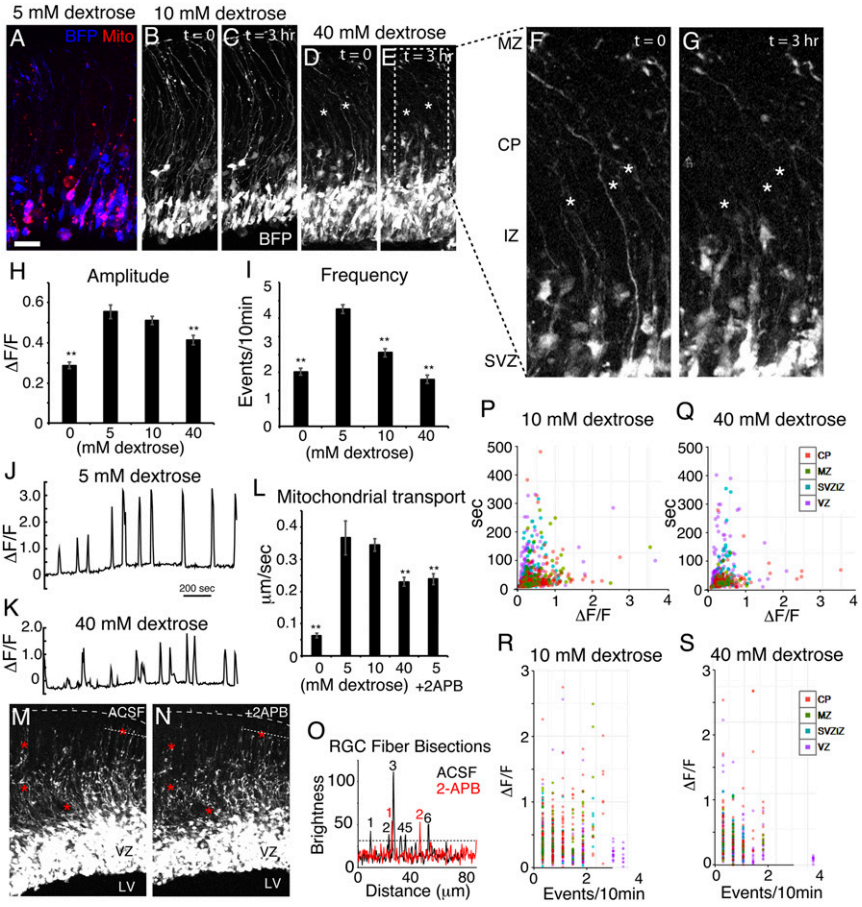

Fig. 4. Hyperglycemia degrades the RGC scaffold, Ca^{2+} signaling, and mitochondrial motility. (*A–G*) BFP Z-stacks of labeled RGCs show retraction (asterisks) of RGC fibers after exposure to 5, 10, and 40 mM glucose ($n = 4$, 5, and 4 slices, respectively). (*H* and *I*) Ca^{2+} activity was severely reduced after a few minutes without glucose and reached a maximum in the euglycemic range (5 to 10 mM), but at 40 mM, it was reduced in amplitude and frequency. (*J* and *K*) Example optogenetic Ca^{2+} signal traces of the same RGC at 5 and 40 mM illustrate the reduced amplitude of signals during hyperglycemia. (*L*) Mitochondrial transport was nearly abolished in the absence of dextrose but showed a maximum at euglycemia and a decrease during hyperglycemia as well as in the presence of 100 μM 2-APB ($n = 3$ slices). RGC fibers showed retraction after exposure to 2-APB (*M* and *N*; red asterisks) and the number of fibers crossing the fine dotted line was reduced by 2-APB (*O*). Calcium event property distributions of RGC ROIs in euglycemia and hyperglycemia by region are plotted in *P–S*. (Scale bar: 30 μm in *A–E*; 10 μm in *F* and *G*.) $^{**}P < 0.0001$.

and Movies S9 and S10). Computational analysis of individual events indicated that large-amplitude, short-duration events were most severely reduced, and that the largest decreases were found in RGC basal fibers (Fig. 4 *P–S* and *SI Appendix*, Fig. S4). Mitochondrial motility was maximal within the euglycemic range (between 5 and 10 mM), but was severely reduced at both 0 and 40 mM (Fig. 4*L*). Motile mitochondria were defined as mitochondria that moved linearly at least 2 μm relative to nearby cellular features within a 40-min movie. Bath application of 2-APB, which inhibits Ca^{2+} release from ER-based intracellular stores, also slowed mitochondrial motility and caused the retraction of RGC scaffold fibers (Fig. 4 *L–O*). Values for percent motile according to dextrose concentration were 0 mM dextrose, 19.0% motile, $n = 58$; 5 mM, 92.8%, $n = 111$; 10 mM, 88.1%, $n = 226$; 40 mM, 52.2%, $n = 69$; and 5 mM + 2-APB, 56.9%, $n = 72$. This, together with the above evidence that high intracellular Ca^{2+} correlates with reduced mitochondrial transport, indicates that Ca^{2+} dynamic activity plays a bimodal role in mitochondrial motility in RGCs, both promoting and reducing motility in a concentration-dependent manner, and is consistent with the hypothesis that glucose concentration modulates mitochondrial transport in part by regulating Ca^{2+} activity.

It has been reported that hyperglycemia can induce mitochondrial fission in cardiac cell culture as part of a cell-death pathway (42, 43). To determine whether hyperglycemia had an effect on mouse RGC ultrastructure, we exposed E13.5 embryo cortices to 5 or 40 mM glucose in oxygenated ACSF for up to 2 h and then performed an electron microscopy study of the developing cortex with 3D reconstruction from serial sections. Despite an extensive search, we did not find ultrastructural evidence of cell death or mitochondrial fission or fusion in hyperglycemic or control embryo brains; developing RGCs and neurons demonstrated normal ultrastructure in all specimens analyzed ($n = 8$; *SI Appendix*, Fig. S5).

Dynamic Ca^{2+} Signaling in Cortical Neural Stem Cells but Not in Induced Pluripotent Stem Cells. To further characterize intrinsic Ca^{2+} dynamic signaling properties of RGCs, we isolated and cultured cortical neural stem cells (NSCs) from E11.5 mouse embryos as previously described (44) (*SI Appendix*, Fig. S6*A*), and labeled them using Fluo4 and Mitotracker Red (*SI Appendix*, Fig. S6*B*). Similar to RGCs labeled with GCaMP5 in cortical slices, mouse cortical NSCs in culture showed abundant Ca^{2+} transients with a wide variety of event properties [$n = 10{,}667$ Ca^{2+} events from 1,843 regions of interest (ROIs), in 10-min movies of $n = 4$ plates; *SI Appendix*, Fig. S6 *C–F* and Movie S11]. Mean amplitude was 24.5 ± 2.5% ΔF/F; duration was 16.6 ± 0.2 s, and frequency was 9.36 ± 0.04 events per 10 min. The most striking Ca^{2+} event property of many of these cells was their rhythmic, pacemakerlike nature (*SI Appendix*, Fig. S6*G*) with a diverse frequency distribution

(*SI Appendix*, Fig. S6*D*). Other NSCs showed only isolated Ca^{2+} events. Pacemaker cells demonstrated various event frequencies (*SI Appendix*, Fig. S6*G*) but were observed only rarely in RGCs in cortical slices, suggesting that the Ca^{2+} state of cultured RGCs is different from that in acute embryonic brain slices. Pacemaker activity was also found in NSCs that did not appear to have any contacts with adjacent cells, and adjacent pacemaker cells were not generally phase locked. Thus, pacemaker Ca^{2+} activity is likely an intrinsic property of cortical NSCs in vitro. Computational analysis revealed ordered activity structure in rasterplot-represented events (*SI Appendix*, Fig. S7), with progression of activity between ROIs, demonstrating that cortex-derived NSCs can assemble into communicating groups of cells, as in the syncytium of the VZ in vivo.

Slow Ca^{2+} activity is a common physiological property of VZ and SVZ progenitors in the developing cortex but is comparatively rare in developing neurons (28). To determine whether other types of stem cells show Ca^{2+} dynamic events, we cultured human induced pluripotent stem cells (iPSCs) and labeled them with the Ca^{2+} indicator Fluo4 (*SI Appendix*, Fig. S6*H*). Compared with cortical NSCs, we observed only very rare Ca^{2+} fluctuations, none of which were oscillatory in nature (n = 1,390 ROIs analyzed from n = 4 plates; *SI Appendix*, Fig. S6 *G* and *I*). Thus, iPSCs and cortical NSCs show strikingly different levels of Ca^{2+} activity, although both populations are highly mitotically active (Movie S13).

Based on our data in RGC fibers showing an inverse relationship between Ca^{2+} concentration and mitochondrial transport rate, we hypothesized that this could also be the case in RGC-derived NSC somata. We examined dual-channel confocal movies and found that mitochondrial movement was inversely correlated with Ca^{2+} pulses (Fig. 5 and Movie S12). We found that groups of RGC mitochondria can move en masse in a coordinated and directed fashion. However, other mitochondria in the same cells did not appear to react to changes in Ca^{2+} levels, indicating the presence of both Ca^{2+}-sensitive and Ca^{2+}-insensitive mitochondrial populations.

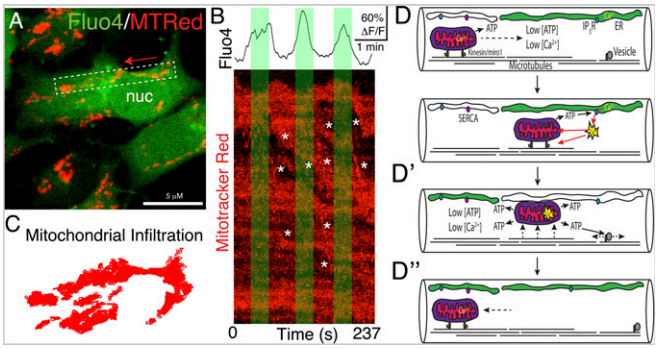

Fig. 5. Mitochondrial motility regulated by cyclical charging/discharging of Ca^{2+} in cortical stem cells. (*A*) High-magnification view of a mouse cortical NSC derived from an E11.5 embryo and labeled with Fluo4 and Mitotracker Red. Mitochondrial movement direction is indicated by a red arrow; see also Movie S12. nuc, nucleus. (*B*) Boxed region in *A* extracted from the dual-channel movie file and converted to a kymograph and related to the Ca^{2+} signal intensity. Rapid mitochondrial movements (asterisks) are more common with lower Ca^{2+} than high Ca^{2+} (green regions) (n = 23 cells from n = 4 plates). Other mitochondria appear unaffected by Ca^{2+} fluctuations. (*C*) Total mitochondrial infiltration of the cell in *A* was captured in a movie and displayed as a scatterplot of the accumulated *xy*-coordinates of mitochondrial ROIs. (*D*) Model of Ca^{2+} regulation of mitochondrial motility. Low Ca^{2+} permits rapid mitochondrial transport along microtubules within RGC fibers. (*D′*) ER Ca^{2+} discharge inactivates mitochondrial transport machinery and promotes ATP production. (*D″*) Ca^{2+} reuptake by ER returns the cytosol to a low Ca^{2+} state, reactivating mitochondrial shuttling. IP_3R, inositol trisphosphate receptor; SERCA, sarco/endoplasmic reticulum Ca^{2+}-ATPase.

Discussion

Determining the physiological mechanisms of RGCs needed for the development of the cortex, as well as their genetic and environmental sensitivities (14), will help shed light on the causes of a variety of congenital neurological diseases and reveal avenues for prevention. In our study, we found an ability of hypo- or hyperglycemia to impair RGC function by uncoupling Ca^{2+} signaling and mitochondrial transport, indicating potential mechanisms by which gestational metabolic disease can cause cortical development disorders in mice. For example, our observation of partial RGC fiber retraction during hyperglycemia in slices can be expected to lead to neuronal migration defects in vivo, including, for example, subcortical band heterotopias, which are occasionally observed in cases of ASD (45). Slowed Ca^{2+} activity can lead to reduced proliferation rates of RGCs (29, 46) and, hence, reduced or delayed neuronal output. Changes in the Ca^{2+} activity code likely have further effects on neuronal differentiation that are not understood at present, but we found that one of these changes—reduced bidirectional signaling in RGC fibers—leads to impaired mitochondrial transport and likely impaired transport of developmental signals such as retinoic acid and mRNA (23, 24) from the pial surface to RGC somata, directing their division and neurogenesis. Reduction of mitochondrial retention in pial and apical endfeet, combined with reduced Ca^{2+} tone by hyperglycemia, would also be expected to impair signaling systems such as the FGF–phospholipase C-γ pathway (28), interfering with the normal self-renewal and differentiation balance of cortical development. Downstream Ca^{2+} signaling targets such as CaMKII are important regulators of gene expression and could similarly be impaired by alterations in RGC Ca^{2+} tone.

While there was a clear association between Ca^{2+} level and the transport rate of many RGC mitochondria, we also found that the transport rate of other mitochondria was unaffected by Ca^{2+} events. The data, therefore, support the existence of two populations of RGC mitochondria: one that is not attached to (or associated with inactive) transport machinery and a second that is. In this model, only directed mitochondrial transport is affected by Ca^{2+} pulsation. Thus, Ca^{2+} activity contributes to an elaborate mitochondrial distribution system in RGCs that functions by disabling mitochondrial transport systems in cellular regions in need of higher metabolic activity. For example, RGC apical endfeet show the highest levels of Ca^{2+} activity within RGC fibers (28), potentially explaining why they are rich in mitochondria (*SI Appendix*, Fig. S5). Indeed, elevated Notch, FGF, and other signaling occurs in apical endfeet (47), consuming large amounts of energy, and it seems likely that FGF signaling indirectly controls mitochondrial enrichment there by elevating Ca^{2+} activity as shown previously (28).

Disrupting either RGC mitochondrial function or (seemingly paradoxically) Ca^{2+} activity correlated with reduced mitochondrial transport (Figs. 3 and 4). In principle, other environmental impairment of this feedback mechanism (e.g., gestational alcohol exposure, maternal inflammation, or ion channel medications) could lead to developmental neurologic disease by altering RGC physiology and function, and such factors should be investigated accordingly. In our model (Fig. 5), we propose that cytoplasmic Ca^{2+} levels below a certain threshold will impair aerobic respiration (32), leading to reduced ATP production needed for local mitochondrial and other transport machinery, slowing transport rates. In neurons, mitochondrial distribution and recruitment to synaptically active sites is known to depend on local Ca^{2+} fluctuations associated with synaptic function; high Ca^{2+} locally derails mitochondria from transport machinery, impeding their transport and ensuring local metabolic support for active synapses (36). It is important to note that repetitive neuronal activity, while 1,000-fold faster than the slow Ca^{2+} activity of RGCs and NSCs observed in this study, similarly achieves an elevated intracellular Ca^{2+} level for localized mitochondrial retention.

Thus, we suggest that the early role of slow-wave Ca^{2+} activity in RGCs and early neuroblasts is later supplanted by action potential-induced Ca^{2+} elevations in mature neurons.

Radial glia are the primary NSC of the central nervous system (48), and, by extension, the Ca^{2+}–mitochondria cross-regulatory mechanisms observed in this study could be in play elsewhere in the brain or spinal cord. It seems possible that maternal hyperglycemia could alter RGC physiology in the diencephalon, resulting in the inheritance of environmentally induced circuitry changes of metabolism regulatory centers.

Studies have indicated that neuronal function is degraded in diseases such as amyotrophic lateral sclerosis, Huntington's disease, and Alzheimer's disease partly due to disrupted mitochondrial transport in axons (49–52). In muscle cells, local ER-based Ca^{2+} elevation also promotes mitochondrial retention, ensuring Ca^{2+} buffering and greater local energy production (33). Thus, this type of feedback may represent a fundamental disease-associated mechanism in many cell types. The variations between Ca^{2+}-based mitochondrial retention systems of developing brain, muscle, and stem cells hint at the evolutionary importance and diverse mechanisms of regulating mitochondrial distribution according to the metabolic and signaling requirements of larger and ever more complex cell types.

Materials and Methods

All animal procedures were conducted according to Yale University Institutional Animal Care and Use Committee policies. In utero electroporation of plasmids containing BFP, GCaMP5, Mito-mCherry, and ER-EGFP in CD1 dams was as described previously (28). Immunohistochemistry for Sox2, Tbr2, BrdU, GLAST, and Casp3 utilized antigen retrieval as described previously (28). HFD feeding was for 3 mo before breeding. Calcium movies utilized a Zeiss LSM 510 confocal microscope with a heated stage, with data processing in ImageJ, MATLAB, and R. For full methods, see *SI Appendix*.

ACKNOWLEDGMENTS. We thank Mariamma Pappy and Marya Shanabrough for technical help; Hitoshi Komuro for helpful discussions; and the Kavli Institute for Neuroscience at Yale University and the National Institutes of Health (NIH Grants DA02399, EY002593, DK111178, and DK045735) for funding.

1. Rakic P (1988) Specification of cerebral cortical areas. *Science* 241:170–176.
2. Lui JH, Hansen DV, Kriegstein AR (2011) Development and evolution of the human neocortex. *Cell* 146:18–36.
3. Dehay C, Kennedy H (2007) Cell-cycle control and cortical development. *Nat Rev Neurosci* 8:438–450.
4. Geschwind DH, Rakic P (2013) Cortical evolution: Judge the brain by its cover. *Neuron* 80:633–647.
5. Ackman JB, Burbridge TJ, Crair MC (2012) Retinal waves coordinate patterned activity throughout the developing visual system. *Nature* 490:219–225.
6. Sur M, Rubenstein JL (2005) Patterning and plasticity of the cerebral cortex. *Science* 310:805–810.
7. Grove EA, Fukuchi-Shimogori T (2003) Generating the cerebral cortical area map. *Annu Rev Neurosci* 26:355–380.
8. Rakic P (1974) Neurons in rhesus monkey visual cortex: Systematic relation between time of origin and eventual disposition. *Science* 183:425–427.
9. Garel S, Huffman KJ, Rubenstein JL (2003) Molecular regionalization of the neocortex is disrupted in Fgf8 hypomorphic mutants. *Development* 130:1903–1914.
10. Bishop KM, Garel S, Nakagawa Y, Rubenstein JL, O'Leary DD (2003) Emx1 and Emx2 cooperate to regulate cortical size, lamination, neuronal differentiation, development of cortical efferents, and thalamocortical pathfinding. *J Comp Neurol* 457: 345–360.
11. Fukuchi-Shimogori T, Grove EA (2001) Neocortex patterning by the secreted signaling molecule FGF8. *Science* 294:1071–1074.
12. Bae BI, et al. (2014) Evolutionarily dynamic alternative splicing of GPR56 regulates regional cerebral cortical patterning. *Science* 343:764–768.
13. Hatten ME (1999) Central nervous system neuronal migration. *Annu Rev Neurosci* 22: 511–539.
14. Stolp HB, et al. (2011) Reduced ventricular proliferation in the foetal cortex following maternal inflammation in the mouse. *Brain* 134:3236–3248.
15. Krakowiak P, et al. (2012) Maternal metabolic conditions and risk for autism and other neurodevelopmental disorders. *Pediatrics* 129:e1121–e1128.
16. Christensen DL, et al. (2016) Prevalence and characteristics of autism spectrum disorder among 4-year-old children in the Autism and Developmental Disabilities Monitoring Network. *J Dev Behav Pediatr* 37:1–8.
17. Barnes-Powell LL (2007) Infants of diabetic mothers: the effects of hyperglycemia on the fetus and neonate. *Neonatal Netw* 26:283–290.
18. DeSisto CL, Kim SY, Sharma AJ (2014) Prevalence estimates of gestational diabetes mellitus in the United States, Pregnancy Risk Assessment Monitoring System (PRAMS), 2007-2010. *Prev Chronic Dis* 11:E104.
19. Napoli E, Wong S, Hertz-Picciotto I, Giulivi C (2014) Deficits in bioenergetics and impaired immune response in granulocytes from children with autism. *Pediatrics* 133: e1405–e1410.
20. Giulivi C, et al. (2010) Mitochondrial dysfunction in autism. *JAMA* 304:2389–2396.
21. Rossignol DA, Frye RE (2012) Mitochondrial dysfunction in autism spectrum disorders: A systematic review and meta-analysis. *Mol Psychiatry* 17:290–314.
22. Frye RE, James SJ (2014) Metabolic pathology of autism in relation to redox metabolism. *Biomark Med* 8:321–330.
23. Siegenthaler JA, et al. (2009) Retinoic acid from the meninges regulates cortical neuron generation. *Cell* 139:597–609.
24. Pilaz LJ, Lennox AL, Rouanet JP, Silver DL (2016) Dynamic mRNA transport and local translation in radial glial progenitors of the developing brain. *Curr Biol* 26:3383–3392.
25. Spitzer NC (2006) Electrical activity in early neuronal development. *Nature* 444: 707–712.
26. Webb SE, Miller AL (2003) Calcium signalling during embryonic development. *Nat Rev Mol Cell Biol* 4:539–551.
27. Berridge MJ (2001) The versatility and complexity of calcium signalling. *Complexity in Biological Information Processing*, Novartis Foundation Symposium 239 (John Wiley & Sons Ltd., Chichester, UK), pp 52–64; discussion 64–67, 150–159.
28. Rash BG, Ackman JB, Rakic P (2016) Bidirectional radial Ca(2+) activity regulates neurogenesis and migration during early cortical column formation. *Sci Adv* 2: e1501733.
29. Weissman TA, Riquelme PA, Ivic L, Flint AC, Kriegstein AR (2004) Calcium waves propagate through radial glial cells and modulate proliferation in the developing neocortex. *Neuron* 43:647–661.
30. Luzzo KM, et al. (2012) High fat diet induced developmental defects in the mouse: Oocyte meiotic aneuploidy and fetal growth retardation/brain defects. *PLoS One* 7: e49217.
31. Vogt MC, Brüning JC (2013) CNS insulin signaling in the control of energy homeostasis and glucose metabolism–From embryo to old age. *Trends Endocrinol Metab* 24:76–84.
32. Rizzuto R, De Stefani D, Raffaello A, Mammucari C (2012) Mitochondria as sensors and regulators of calcium signalling. *Nat Rev Mol Cell Biol* 13:566–578.
33. Yi M, Weaver D, Hajnóczky G (2004) Control of mitochondrial motility and distribution by the calcium signal: A homeostatic circuit. *J Cell Biol* 167:661–672.
34. Martinvalet D (2018) The role of the mitochondria and the endoplasmic reticulum contact sites in the development of the immune responses. *Cell Death Dis* 9:336.
35. van Vliet AR, Agostinis P (2018) Mitochondria-associated membranes and ER stress. *Curr Top Microbiol Immunol* 414:73–102.
36. MacAskill AF, Kittler JT (2010) Control of mitochondrial transport and localization in neurons. *Trends Cell Biol* 20:102–112.
37. Miller KE, Sheetz MP (2004) Axonal mitochondrial transport and potential are correlated. *J Cell Sci* 117:2791–2804.
38. Leblanc OH, Jr (1971) The effect of uncouplers of oxidative phosphorylation on lipid bilayer membranes: Carbonylcyanidem-chlorophenylhydrazone. *J Membr Biol* 4: 227–251.
39. O'Shaughnessy K, Hladky SB (1983) Transient currents carried by the uncoupler, carbonyl cyanide m-chlorophenylhydrazone. *Biochim Biophys Acta* 724:381–387.
40. Bozzetti P, et al. (1988) The relationship of maternal and fetal glucose concentrations in the human from midgestation until term. *Metabolism* 37:358–363.
41. Bondy C, Werner H, Roberts CT, Jr, LeRoith D (1992) Cellular pattern of type-I insulin-like growth factor receptor gene expression during maturation of the rat brain: Comparison with insulin-like growth factors I and II. *Neuroscience* 46:909–923.
42. Yu T, Robotham JL, Yoon Y (2006) Increased production of reactive oxygen species in hyperglycemic conditions requires dynamic change of mitochondrial morphology. *Proc Natl Acad Sci USA* 103:2653–2658.
43. Yu T, Sheu SS, Robotham JL, Yoon Y (2008) Mitochondrial fission mediates high glucose-induced cell death through elevated production of reactive oxygen species. *Cardiovasc Res* 79:341–351.
44. Adepoju A, Micali N, Ogawa K, Hoeppner DJ, McKay RD (2014) FGF2 and insulin signaling converge to regulate cyclin D expression in multipotent neural stem cells. *Stem Cells* 32:770–778.
45. Stoner R, et al. (2014) Patches of disorganization in the neocortex of children with autism. *N Engl J Med* 370:1209–1219.
46. Malmersjö S, Rebellato P, Smedler E, Uhlén P (2013) Small-world networks of spontaneous Ca(2+) activity. *Commun Integr Biol* 6:e24788.
47. Hatakeyama J, et al. (2014) Cadherin-based adhesions in the apical endfoot are required for active Notch signaling to control neurogenesis in vertebrates. *Development* 141:1671–1682.
48. Rakic P (2009) Evolution of the neocortex: A perspective from developmental biology. *Nat Rev Neurosci* 10:724–735.
49. Miller KE, Sheetz MP (2006) Direct evidence for coherent low velocity axonal transport of mitochondria. *J Cell Biol* 173:373–381.
50. Gunawardena S, Goldstein LS (2001) Disruption of axonal transport and neuronal viability by amyloid precursor protein mutations in *Drosophila*. *Neuron* 32:389–401.
51. Gunawardena S, et al. (2003) Disruption of axonal transport by loss of huntingtin or expression of pathogenic polyQ proteins in *Drosophila*. *Neuron* 40:25–40.
52. Hurd DD, Saxton WM (1996) Kinesin mutations cause motor neuron disease phenotypes by disrupting fast axonal transport in *Drosophila*. *Genetics* 144:1075–1085.